

# COMPARISON OF NEAR INFRARED SPECTROSCOPY (NIRS) SIGNAL QUANTITATION BY MULTILINEAR REGRESSION AND NEURAL NETWORKS

A. Martinez-Coll, H.T. Nguyen

Key University Research Strength in Health Technologies

University of Technology, Sydney; PO Box 123, Broadway, NSW 2007, AUSTRALIA

**Abstract-** Signal quantitation in most near infrared spectroscopy (NIRS) instruments is achieved through solving simultaneous equations or multiple regression analysis. The aim of this study was to compare NIRS signal quantitation by conventional multiple regression to artificial neural networks. Sixteen adult sheep were used in the study of the effects of changes in cerebral blood flow and metabolism through induction of seizures, ischemia, and hypercapnia. NIRS-derived signal attenuation for relative blood volume (BV) and oxygen desaturation (DESAT) were compared to simultaneous blood flow values measured by laser Doppler flowmetry and venous oxygen saturation (SvO<sub>2</sub>) determined from direct blood gas analysis. The regression for flow provided a zero p-value, a variance S=17.57 and F statistic=50.49. The residuals vs. fits plots suggest that the current model would underestimate values below the mean and overestimate those above the mean. An improved regression model for SvO<sub>2</sub> provided a zero p-value, a variance S=14.1 and F statistic=4.26. Two different neural networks were implemented for flow and oxygen saturation. Both networks “tracked” their values closely and with low cycle errors. Neural networks are powerful tools for evaluation of rapidly changing, variable environments.

**Keywords** - Near infrared spectroscopy, regression, neural network

## I. INTRODUCTION

Near infrared spectroscopy (NIRS) is a technique that relies on the relative transparency of biological tissues to light in the 600-1000nm range, as well as on compounds (or chromophores) whose absorption spectra is oxygen status dependent (mainly oxy- and deoxygenated hemoglobin, and the redox state of cytochrome aa3) [1]. Despite the widespread use of the technology to monitor tissue hemodynamics and oxygenation levels, its clinical acceptance is still elusive. Absolute signal quantitation depends on the knowledge of the distance traveled by the photons between emission and detection, the total pathlength. Biological tissues are inhomogeneous media where multiple scattering events occur, resulting in longer pathlengths than the distance between emitter and detector. Mathematical techniques such as Monte Carlo simulations have led to the derivation of a wavelength-dependent differential pathlength factor (DPF) for various tissues [2]. The DPF represents a probabilistic average distance traveled by the photons. The various NIRS algorithms either utilise multilinear regression or simultaneous equations and the DPF to obtain wavelength multipliers and allow absolute signal quantitation [3]. However, their effectiveness is questionable in conditions of physiologic stress (as in vasoconstriction or vasodilatation) which alter tissue geometry.

Mean pial artery dilatation of 18-29% have been reported during hypoxia [4]. The change in diameter would result in a redistribution of the proportion of blood volume in the arterial vascular compartment; and therefore, of oxyhemoglobin. These

rapid, dynamic changes can lead to significant errors in signal quantitation.

The following study describes the use of NIRS during direct cortical measurements from the brain of signal attenuation at various wavelengths (760nm, 800nm, 830nm, 850nm, and 980nm) during induced changes in cerebral blood flow and oxygenation levels. Correlations were obtained for NIRS BV and DESAT with independent measurements of regional cerebral blood flow and venous oxygen saturation. Prediction of blood flow and SvO<sub>2</sub> from NIRS data were calculated by both multilinear regression models as well as artificial neural networks.

## II. METHODOLOGY

Following approval from the Royal North Shore Hospital Animal Care and Ethics Committee (ACEC), sixteen adult Merino Cross ewes with an average body weight of 48.4 +/- 5.3 Kg were used in the study. In some instances, multiple episodes of a particular protocol were carried out on the same animal.

### Anesthesia

The animals were anesthetized with pentothal (1g/20 ml) as induction, intubated with a cuffed tracheal tube (10 mm ID), and ventilated 1 l/min oxygen (>40%), 2 l/min nitrogen dioxide (52%), and halothane (1%) through a respirator (Bird model 8; Bird Australia, Pty. Ltd., Chatswood, NSW, Australia). The respiratory parameters were monitored and adjustments were made (in tidal volume, and/or respiratory rate) when necessary to maintain an expired CO<sub>2</sub> partial pressure of ~ 40 mmHg. Maintenance fluid was provided through peripheral venous access with 0.9% NaCl. Anesthesia was maintained with a continuous fentanyl drip (10µg/ml) at 30 ml/kg for the first 30 minutes and then changed over to 20 ml/kg for the remainder of the procedure. Electrocardiography was monitored with electrodes clipped to the extremities.

### Surgery

After wool was removed from the neck and thigh area, incisions were made along both sides of the trachea and both carotids arteries isolated and loosely fitted with rubber ties. The left jugular vein was used for insertion of a dual cannula for central venous pressure monitoring and IV drug administration. A similar procedure was followed to isolate both femoral arteries. An arterial cannula was placed in the left femoral for blood sampling and blood pressure monitoring. The right femoral was used to insert a cannula for blood pressure reduction through

## Report Documentation Page

<b>Report Date</b> 25OCT2001	<b>Report Type</b> N/A	<b>Dates Covered (from... to)</b> -
<b>Title and Subtitle</b> Comparison of Near Infrared Sepctroscopy (NIRS) Signal Quantitation by Multilinear Regression and Neural Networks		<b>Contract Number</b>
		<b>Grant Number</b>
		<b>Program Element Number</b>
<b>Author(s)</b>	<b>Project Number</b>	
	<b>Task Number</b>	
	<b>Work Unit Number</b>	
<b>Performing Organization Name(s) and Address(es)</b> Key University Research Strength in Health Technologies University of Technology, Sydney; PO Box 123, Broadway, NSW 2007, AUSTRALIA		<b>Performing Organization Report Number</b>
<b>Sponsoring/Monitoring Agency Name(s) and Address(es)</b> US Army Research, Development & Standardization Group (UK) PSC 802 Box 15 FPO AE 09499-1500		<b>Sponsor/Monitor's Acronym(s)</b>
		<b>Sponsor/Monitor's Report Number(s)</b>
<b>Distribution/Availability Statement</b> Approved for public release, distribution unlimited		
<b>Supplementary Notes</b> Papers from the 23rd Annual International Conference of the IEEE Engineering in Medicine and Biology Society, October 25-28, 2001, held in Istanbul, Turkey. See also ADM001351 for entire conference on cd-rom., The original document contains color images.		
<b>Abstract</b>		
<b>Subject Terms</b>		
<b>Report Classification</b> unclassified	<b>Classification of this page</b> unclassified	
<b>Classification of Abstract</b> unclassified	<b>Limitation of Abstract</b> UU	
<b>Number of Pages</b> 4		

the removal of blood. Body temperature was monitored by a rectal temperature probe.

The animal was turned over and placed in a prone position with the legs stretched and secured to the operating table; the head was also secured in a specially designed head holder. After shaving the head, a midline incision was made, the skin reflected and the skull exposed. Burr holes were drilled on opposite sides of the skull as well as caudally from the sagittal suture. The size of the holes was then adjusted to allow fixation of both the laser Doppler flowmeter and NIRS probes. The third burr hole was used for cannulation of the sagittal sinus (SS) for direct venous sampling.

### *Instrumentation*

#### *Laser Doppler flowmeter and NIR spectrometer-*

Cerebral blood flow was monitored with an ALF21 laser Doppler flowmeter (Advance Co., Ltd, Japan). It offers non-destructive and continuous monitoring of blood flow (range 0-100 ml/min/100g) on various sites in the body, like skin, stomach mucosa, brain, and intestine surfaces. It relies on a low-power output semiconductor laser (780 nm with an optical power output of <2mW) and provides measurements of fine tissue blood flow such as capillary flow, using a 1mm diameter half-spherical probe.

The research NIRS instrument consists of five 1 watt solid state lasers (780, 800, 830, 850, and 980 nm) fired sequentially at 5μs pulses for a 1 ms cycle, and a 5 mm<sup>2</sup> photodiode receiver. In vitro assessment of the instrument has been previously reported [5]. The optode separation used for these studies was 0.5 cm.

The signals from the LDF and NIRS instrument, arterial and venous pressures, and ECG were connected to a MacLab 16S data acquisition module running Chart 3.5.6 software (AD Instruments, Castle Hill, Australia) at a sampling rate of 4 Hz. A fluid filled pressure transducer was used to monitor central venous pressure, while a 5F Millar catheter-tip manometer (Millar Instruments, Inc., Houston, TX) provided arterial pressure recordings. The pressure signals were amplified (System 6; Triton Technology, Inc., San Diego, CA) and recorded with the MacLab analog-to-digital converter. The MacLab hardware and software provided the option for continuous display and recording of all channels.

#### *Cerebral blood flow response to hypercapnia*

Cerebral blood flow was increased by introduction of 5% CO<sub>2</sub> into the breathing circuit for 4 minutes and then turned off. In some animals more than one CO<sub>2</sub> inhalation episode was carried out.

### *Seizures*

Changes in regional cerebral blood flow and oxygen consumption were induced by topical application of 500 mg of ampicillin subdurally through the SS cannula puncture. Penicillin-induced seizures peak at around 3 minutes after application and resolve spontaneously [6].

### *Ischemia*

Global cerebral ischemia was implemented through hypotension and bilateral carotid occlusion as described by Smith and collaborators [7]. Following a stabilization period, blood gas samples (both arterial and venous) are taken prior to the removal of blood through hemorrhage. Once MAP reaches < 50 mmHg, the hemorrhage is stopped to maintain that level of arterial pressure. At this point the carotids ties are pulled and tightened in place with alligator forceps to completely occlude flow.

After a period of 4 minutes of complete carotid occlusion, the ties are released and the response observed for the next 5 minutes. Changes in NIRS and LDF are recorded continuously during the whole ischemic episode. Ischemia was followed by a 10 minute period of reperfusion. Data gathering ceased at the end of reperfusion and the animals were euthanased with an intravenous bolus of KCL (3g).

### *Statistical Analysis*

The data recorded throughout the whole study were used to implement separate multiple regression models for LDF and SvO<sub>2</sub>, based exclusively on NIRS wavelength attenuation data (at 780 nm, 850 nm, 980 nm, 800 nm, 830 nm, DESAT, and BV). The model's variance (S), F statistic, and the corresponding regression equations were obtained. A p-value < 0.05 was considered significant.

### *Neural network*

Two separate neural networks are described, one for prediction of SvO<sub>2</sub> and the other for LDF. A standard feedforward architecture with 10 inputs (nine from experimental data and one as a bias), a number of hidden nodes and a single output was implemented. The network was trained with results obtained from three sheep and validated in one. Initially, network weight matrices were randomly assigned. After training, the final weight matrices were obtained and used for validation. The inputs for each network were selected according to their expected influence on the predicted parameter.

## III. RESULTS

### *Correlation between NIRS wavelengths and absolute flow values*

Multilinear regression model- Subset regressions were carried out to determine the effect of NIRS wavelength data on absolute flow values, as measured by LDF from all animals. These results show that the single-best predictor for LDF is  $\lambda_{850}$ . However, the best two predictors were  $\lambda_{850}$  and  $\lambda_{800}$ . A multiple regression model using the spectrometer data exclusively to determine flow showed that the predictors were not significant to measured LDF values; however, the overall regression provided a zero p-value, a variance S=17.57, and F statistic = 50.49. The regression equation was  $LDF = 25.15 * (780 \text{ nm}) + 3.14 * (850 \text{ nm}) + 10.24 * (980 \text{ nm}) - 6.77 * (800 \text{ nm}) + 7.59 * (830 \text{ nm}) + 3.78 * (DESAT) - 3.87 * (BV)$ .

The pattern shown in the residuals vs. fits plots suggests that the current model would underestimate values below the mean while overestimate those above the mean, as shown in Figure 1A.

Neural network model- A network with three hidden neurons was set up to predict LDF values from SvO<sub>2</sub>, MAP and NIRS parameters. Due to the necessary augmentation of inputs and of the hidden layer by one fixed input to account for bias (or offset), this neural network should have 10 input neurons, four hidden neurons, and one output neuron.

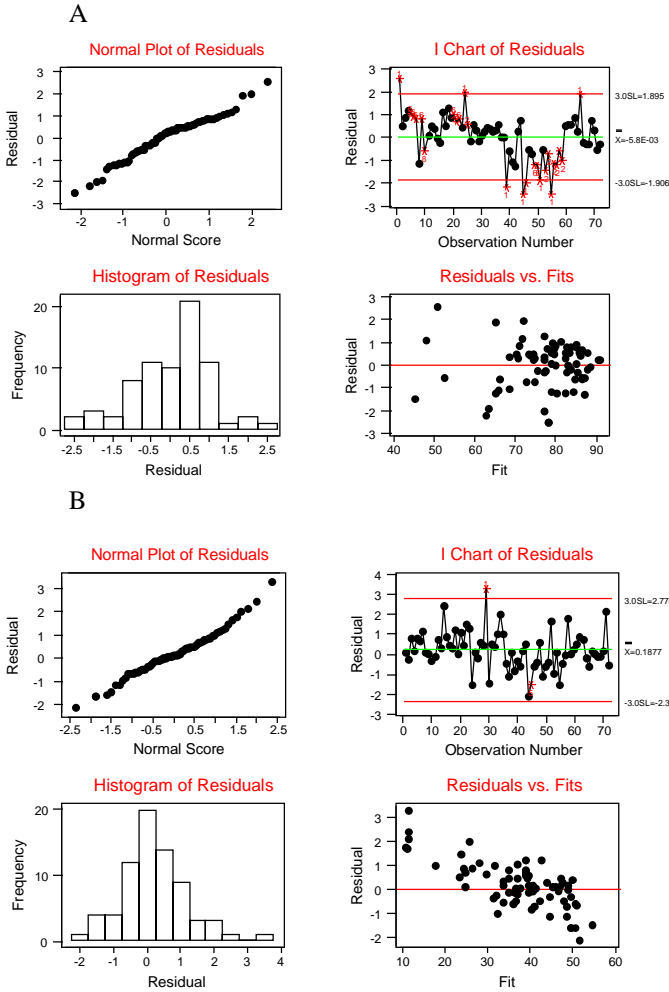


Figure 1: Multilinear regression plots for A) flow, and B) SvO<sub>2</sub>.

There are two weight matrices for the neural network: the hidden layer weight matrix  $\bar{\mathbf{W}}(3 \times 10)$  and the output layer weight matrix  $\mathbf{W}(1 \times 4)$ . This neural network is trained using the back-propagation learning algorithm in which synaptic strengths are systematically modified using negative gradient descent so that the response of the network increasingly approximates the command from the user. Although the cycle error for the training set decreased very quickly after ~ 50 cycles, it did not seem to continue to decrease significantly after 500 cycles. The profile for the training set shows that the network was accurate in “tracking” LDF values (Figure 2A).

The final output layer weight matrix  $\mathbf{W}$  and hidden layer weight matrix  $\bar{\mathbf{W}}$  are:

$$\mathbf{W} = \begin{bmatrix} 0.6844 & 0.0571 & 0.1652 & -1.1268 \end{bmatrix}$$

$$\bar{\mathbf{W}} = \begin{bmatrix} 0.7657 & -0.5754 & \cdots & 0.1453 \\ -1.7547 & 1.8148 & \cdots & 1.1338 \\ -1.6911 & 1.5662 & \cdots & 1.1035 \end{bmatrix}$$

#### Correlation between NIRS wavelengths and SvO<sub>2</sub>

Multilinear regression- The results show that the single-best predictor for SvO<sub>2</sub> is  $\lambda_{980}$ . The best two predictors were  $\lambda_{780}$  and  $\lambda_{980}$ . The multiple regression model to determine SvO<sub>2</sub> showed that the predictors were not significant to measured SvO<sub>2</sub> values (see Figure 1B); however, the overall regression (with the addition of a constant) provided a zero p-value, a variance  $S=14.1$ , and F statistic = 4.26. The regression equation was  $\text{SvO}_2 = 92.6 + 95.3 * (780 \text{ nm}) - 40 * (850 \text{ nm}) - 45.78 * (980 \text{ nm}) - 12.62 * (800 \text{ nm}) - 4.16 * (830 \text{ nm}) - 55 * (\text{DESAT}) - 18.21 * (\text{BV})$ .

Neural network model- As with LDF, a neural network with was implemented to predict SvO<sub>2</sub> from LDF, MAP and NIRS parameters. This time, the model used five hidden neurons. Due to the necessary augmentation of inputs and of the hidden layer by one fixed input to account for bias (or offset), this neural network should have 10 input neurons, six hidden neurons, and one output neuron. There are two weight matrices for the neural network: the hidden layer weight matrix  $\bar{\mathbf{W}}(5 \times 10)$  and the output layer weight matrix  $\mathbf{W}(1 \times 6)$ . Again, this neural network is trained using the back-propagation learning algorithm and negative steepest descent. The learning algorithm modifies both the output layer weight matrix  $\mathbf{W}$  and the hidden layer weight matrix  $\bar{\mathbf{W}}$  so that the error value decreases.

The SvO<sub>2</sub> training set showed that the network “tracked” the SvO<sub>2</sub> values quite well, with the cycle error considerably decreased after only ~100 cycles and further decreased with increasing number of cycles (Figure 2B).

The final output layer weight matrix  $\mathbf{W}$  and hidden layer weight matrix  $\bar{\mathbf{W}}$  are:

$$\mathbf{W} = \begin{bmatrix} -1.3019 & -2.0837 & 2.1643 & 1.6472 & 0.4030 & 0.7990 \end{bmatrix}$$

$$\bar{\mathbf{W}} = \begin{bmatrix} 2.2668 & -0.3509 & \cdots & 1.1672 \\ -2.6480 & -1.2321 & \cdots & -0.3634 \\ 2.0094 & -1.6209 & \cdots & 3.4345 \\ -1.5036 & 0.4782 & \cdots & 0.8145 \\ 2.3323 & 1.6760 & \cdots & -1.9186 \end{bmatrix}$$

#### IV. DISCUSSION

The best multilinear regressions had significant shortcomings with regards to underestimates for flow values below the mean, as well as overestimates for those values above the mean.

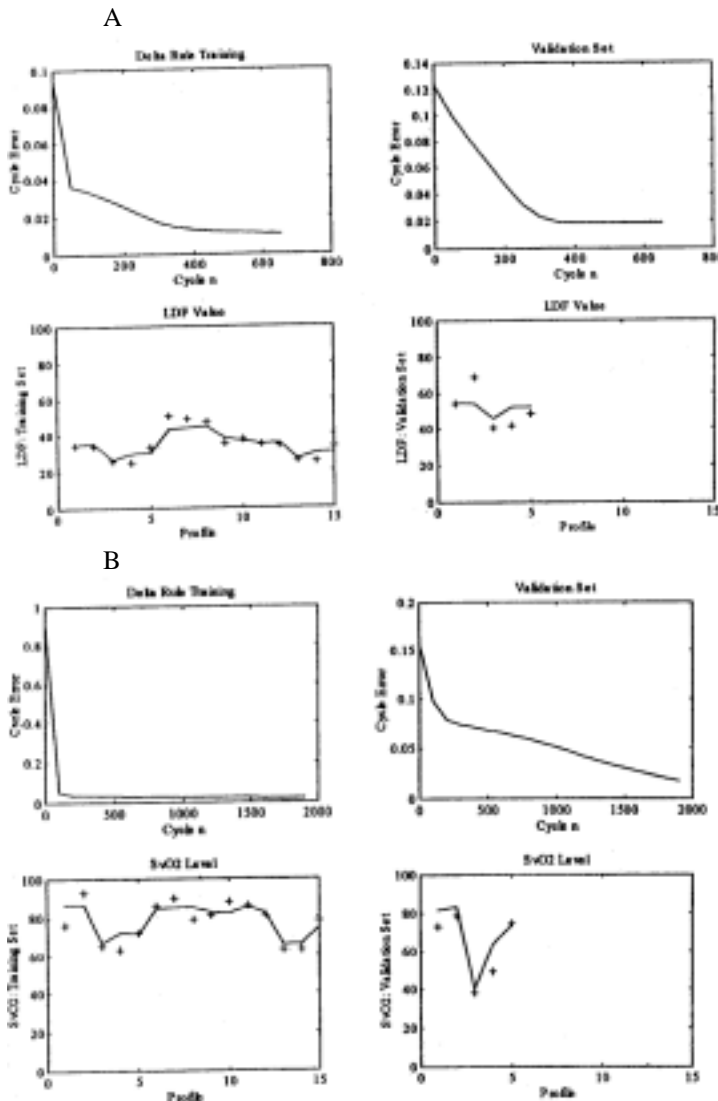


Figure 2: Neural network output for A) flow, and B) SvO<sub>2</sub>.

The neural networks implemented in this study are not in final form; however, they do show that simple static algorithms cannot accurately describe the wide variability of physiological responses between subjects. Additional training of the network will further reduce the error. Predicting SvO<sub>2</sub> using the network proved more accurate than flow. The response for SvO<sub>2</sub> in all animals was consistently similar during each experimental block, ie. before and during seizures, pre-ischemia, at the end of ischemia, and 4 minutes post reperfusion after ischemia.

Despite the actual differences in values, the pattern for SvO<sub>2</sub> was the same in all animals, however, this was not the case with LDF. Although the flow values also correspond with the points in time during which SvO<sub>2</sub> values were obtained, the flow response is not as predictable as the SvO<sub>2</sub> response. Specifically, in the animal used for validation of LDF, the pattern of LDF is different from that seen in the training set. Despite these differences, the network does a good job in tracking LDF.

Obviously, the data gathering and training of the network does require careful preparation and a strict research protocol.

However, once the appropriate training set is implemented with a significant number of subjects, the network should be able to cope with most of the possible permutations and provide fairly accurate values for the "predicted" parameters.

Signal quantification achieved through the implementation and training of artificial neural networks is more accurate, and flexible than algorithms obtained through multiple regression models. Because of the high spatial variability of cerebral blood flow, its quantification is less accurate than that of SvO<sub>2</sub>. Through neural networks, it is possible to predict absolute flow and venous oxygen saturation values without any input from the physical properties of light transport in tissue (eg multiple scattering, depth of penetration of photons, superficial tissues and boundary layers, etc.) with much higher accuracy than multiple regression methods. Testing of the network on the rest of the data will allow determination of its sensitivity and specificity.

## V.CONCLUSION

In the ever changing physiological environment, neural networks prove significantly more accurate than multilinear regression methods used for NIRS signal quantification of cerebral blood flow and oxygen consumption.

## ACKNOWLEDGMENT

This study was funded by a Northern Sydney Area Health Services seeding grant (No.97:13). The authors wish to thank Dr. Peter Petocz from the Mathematics Department for his role in the statistical analysis.

## REFERENCES

1. F. Jöbsis, "Noninvasive infrared monitoring of cerebral and myocardial oxygen sufficiency and circulatory parameters," *Science*, vol. 198, pp. 1264-1267, 1977.
2. D. Delpy, M. Cope, P. van der Zee, S. Arridge, S. Wray, and J.S. Wyatt, "Estimation of optical pathlength through tissue from direct time of flight measurements," *Phys. Med. Biol.*, vol. 33(12), pp. 1433-1442, 1988.
3. S. Matcher, C. Elwell, C. Cooper, M. Cope, and D. Delpy, "Performance comparison of several published tissue near-infrared spectroscopy algorithms," *Analytical Biochem.*, vol. 227, pp. 54-68, 1995.
4. C. Haller and W. Kuschinsky, "Moderate hypoxia: reactivity of pial arteries and local effect of theophylline," *J. Appl. Physiol.*, vol. 63, pp. 2208-2215, 1987.
5. A. Martinez-Coll, P. Cooper, G. Murphy, and H. Nguyen, "Assessment of a laser-powered multiwavelength near-infrared spectrometer," in *Proceedings to the 19th International Conference IEEE/EMBS*, vol. 2, pp. 696-699, 1997.
6. H. Garretson, K. Reid, C. Shields, and J. Noonan, "The effect of topical application of antibiotics on the cerebral cortex: An experimental update," *J. Neurosurg.*, vol. 50, pp. 792-797, 1979.
7. M. Smith, et al., "Models for studying long-term recovery following forebrain ischemia in the rat. 2. A 2-vessel occlusion model," *Acta Neurol. Scand.*, vol. 69, pp. 385-401, 1984.